Metallogr. Microstruct. Anal. (2015) 4:481–487
DOI 10.1007/s13632-015-0246-9

TECHNICAL ARTICLE

Shape Transformation of Bimetallic Au–Pd Core–Shell Nanocubes to Multilayered Au–Pd–Au Core–Shell Hexagonal Platelets

Nabraj Bhattarai[1] · **Tanya Prozorov**[1]

Received: 18 May 2015 / Revised: 19 October 2015 / Accepted: 19 October 2015 / Published online: 5 November 2015

Abstract Transformation of metallic or bimetallic (BM) nanoparticles (NPs) from one shape to another desired shape is of importance to nanoscience and nanotechnology, where new morphologies of NPs lead to enhancement of their exploitable properties. In this report, we present the shape transformation of Au octahedral NPs to Au–Pd core–shell nanocubes, followed by their transformation to nanostars and finally to multilayered Au–Pd–Au core–shell hexagonal platelets in the presence of T30 DNA. The weaker binding affinity of T30 DNA directs the growth to favor the formation of lower energy {111} facets, changing the morphology from nanocubes to nanostar. The nanostars, exhibiting unusual intermediate morphologies, are comprised two sets of shell layers and have Au core, Pd intermediate shell, and Au outer shell. Similarly, the hexagonal platelets, which also have Au core and inner Pd shell, are encased in an external gold shell. The formation of multilayered Au–Pd–Au core–shell hexagonal platelets from Au–Pd core–shell nanocubes via the multilayered nanostars is monitored using scanning/transmission electron microscopy analysis.

Keywords Core–shell nanoparticles · Bimetallic · Multilayered · Au–Pd · DNA-mediated growth

This article is an invited paper selected from presentations at the 2014 Microscopy & Microanalysis Conference, held August 3–7, 2014, in Hartford, Connecticut, USA, and has been expanded from the original presentation.

✉ Nabraj Bhattarai
nabrajbhattarai@ameslab.gov

[1] Emergent Atomic and Magnetic Structures, Division of Materials Sciences and Engineering, Ames Laboratory, Ames, IA 50011, USA

Introduction

The properties and applications of nanoparticles (NPs) strongly depend on their shape, size, and crystalline structure, and the fabrication of NPs with well-controlled shape, size, and crystallinity with sufficient yield is one of the main challenges of the nanoscience and nanotechnology. Bimetallic (BM) NPs comprised two different metals, shown to yield completely new optical, electrical, and catalytic properties compared to their monometallic counterparts, can find applications in optoelectronics, catalysis, drug delivery, solar energy conversions, semiconductors, electronic materials, and numerous other uses [1–5]. Au–Pd core–shell BM NPs are widely used as supported catalysts in several industrial processes [6–9]. Some reactions are catalytically enhanced by utilizing the NPs with specific morphology, corresponding to the prevalence of certain crystallographic faces; hence the synthesis of nanocrystals having definite morphology and crystallographic faces is of importance for practical applications [10–12].

Despite the tremendous interest in the shape- and size-specific synthesis of BM NPs, the rational engineering of heterometallic shells and morphologies remains largely unexplored [13, 14]. The ability to design and fabricate multiple-layered core–shell nanostructures with various metals of interest in controllable manner is ought bring about the enhanced synergetic effects changing the overall properties of the original nanomaterials, and there is always high possibility of getting interesting properties from the synergetic combination of present metals and their crystalline structures. Moreover, the formation of new shapes can be tailored for wider range applications in comparison to the original shape. One facile strategy of controlling the NP morphology employs various DNA molecules in the

reaction [15–18]. It is believed that the DNA hybridization to the surface of the original NPs provides scaffolds or templates for the shell growth and directly affects the morphology and the exploitable properties of the resultant NPs [19–22], as evidenced by the growing number of reports on shape-specific synthesis of NPs utilizing various DNA molecules [23, 24]. We focused on the well-characterized synthesis of Au–Pd NPs in the presence of T30 DNA molecules based on reported the distinct morphology of the particles with star-like shapes [22].

In this report, we present the morphology transformation of Au–Pd core–shell nanocube to Au–Pd–Au multiple-layered core–shell six (6)-cornered nanostar to hexagonal nanometer-sized platelets by introducing the T30 DNA molecules to the synthesis process. While the use of T30 DNA in the synthesis has been reported in the literature, it was not utilized for the synthesis of multilayered nanostructures [23]. The Au NPs were synthesized via the seed-mediated growth process and converted to Au–Pd core–shell nanocubes, which were then transformed into Au–Pd–Au core–shell multilayered nanostars, and finally to hexagonal platelets, in the presence of T30 DNA molecules. We monitored each step of the NP morphology transformation using scanning transmission electron microscopy (STEM) analysis and discussed a possible reaction pathway. The morphologies of NPs grown in the presence of T30 DNA are compared to those obtained without DNA.

Experimental Details

Potassium tetrachloropalladate (K_2PdCl_4), gold(III) chloride trihydrate ($HAuCl_4{\cdot}3H_2O$), hexadecyltrimethylammonium bromide (CTAB), sodium borohydride ($NaBH_4$), and L-ascorbic acid (AA, 99%) were purchased from Sigma-Aldrich and used as received. T30 DNA oligodeoxyribonucleotides were purchased from Integrated DNA Technologies (Coralville, IA) and used as it is received. All aqueous solutions were prepared with deionized water passed through a Millipore Milli-Q Plus water purification system ($\rho = 18.2$ MΩ cm).

Nanoparticle Synthesis

The NPs were fabricated via the seed-mediated growth process in four steps by modifying the reported experimental protocols [25, 26]. In brief, 3–5 nm single-crystal Au seeds were synthesized and grown to ~12 nm octahedral Au NPs, and then it transformed to Au–Pd core–shell nanocubes via the addition of Pd precursor and subsequent reduction by ascorbic acid (AA). The obtained core–shell NPs were incubated with DNA molecules, mixed with additional Au precursor, and reduced by AA forming multilayered Au–Pd core–shell nanostars with 6 corners.

Step 1: Synthesis of Au Seeds

Au seeds were synthesized by combining 75 mM of CTAB with 9 mL of nanopure water and adding 1 mL of 2.5 mM $HAuCl_4$ to maintain that the volume of 10 mL. The Au-CTAB solution was reduced by adding freshly prepared $NaBH_4$ (10 mM, 0.6 mL) while stirring vigorously. The reaction was allowed to continue under slow stirring for 3 h, after which time the reaction volume color changed from yellow to brown. The formation of Au seeds was verified via the TEM examination.

Step 2: Synthesis of Octahedral Au NPs

The Au seeds obtained in **step 1** were grown to 12 nm octahedral Au NPs as follows. *Solution 1* was prepared by diluting 1 mL of solution containing Au seeds with 25 mL of water. In a separate flask, *solution 2* was prepared by adding 0.1457 g of CTAB in 10 mL water. The solution was heated to ~40 °C until it became transparent, mixed with 0.1 mL Au precursor (10 mM $HAuCl_4$), and was further diluted to 25.5 mL. The solution turned to colorless upon addition of AA (0.1 M, 1.5 mL) into the reaction flask. Finally, 1 mL of the seed *solution 1* was added to *solution 2* and stirred for 8 h to obtain a pink-colored solution. Growth of Au seeds into larger Au particles was confirmed by STEM.

Step 3: Synthesis of Au–Pd Core–Shell NPs

Au–Pd core–shell NPs were obtained by adding Pd precursor (K_2PdCl_4 (10 mM)) to the solution containing Au octahedral NPs prepared in **step 2** using the AA as a reducing agent. In this study, the core–shell Au–Pd nanocubes were prepared by adding 0.1 mL of 10 mM K_2PdCl_4 to 5 mL of Au NPs prepared in the previous step and reduced using 0.5 mL of 0.1 M AA. The size of the formed shell was controlled by the amount of Pd precursor added. The formation of core–shell structures was confirmed by HAADF-STEM imaging utilizing Z-contrast difference between Au and Pd.

Step 4: Synthesis of Au–Pd–Au Multilayered Core–Shell Nanostars and Hexagonal Platelets

Following the pioneering work by Lu and coworkers [23], the Au–Pd core–shell nanocubes were transformed into multilayered core–shell Au–Pd–Au nanostars by consequent incubation of Au–Pd core–shell nanocubes obtained in **step 3** with the T30 DNA, followed by introduction of

additional Au precursor, and reduction by AA. In this study, 2 mL of solution containing AuPd nanocubes were centrifuged, diluted to remove the excess CTAB, and incubated with 4 μL (0.2 mM) of T30 DNA for 30 min to allow for the DNA hybridization to the NP surface. $HAuCl_4$ precursor (0.5 mM, 500 μL) was then added to the solution of AuPd nanocubes hybridized with the T30 DNA and incubated for 30 min, after which AA (0.1 M, 0.5 mL) was added as the reducing agent. The reaction was allowed to proceed for 5 h under slow stirring. The obtained colloidal solution was centrifuged 4 times at 5000 rpm for 5 min and subjected to the STEM analysis.

Step 5: Synthesis of Au–Pd–Au Multilayered Core–Shell Without DNA Molecules (Control Experiment)

In a control experiment, AuPdAu multilayered core–shell NPs were synthesized in the manner similar to described in **step 4** without using T30 DNA. Typically, 1 mL of AuPd core–shell NPs are mixed with $HAuCl_4$ precursor (10 mM, 20 μL) and then reduced by AA (0.1 M, 0.5 mL), and the reaction was allowed to continue for 4 h. Formation of the resultant well-developed multilayered core–shell NPs with Au core, Pd intermediate shell, and Au outer shell NPs was monitored by the STEM analysis.

STEM Characterization

Preparation of specimen for the STEM analysis consisted of placing a drop of colloidal NPs on the QuantiFoil™ carbon grids and allowing them to dry at room temperature. The STEM images of the specimen were acquired for each preparatory step using the FEI Tecnai G^2 F20 (S)TEM operating at 200 kV in bright-field TEM mode (BF-TEM) and high angle annular dark field-STEM (HAADF-STEM) modes, equipped with energy dispersive x-ray spectroscopy (EDS) detector and Tridium Gatan image filter.

Results and Discussion

The reduction of Au precursors with strong reducing agent, such as $NaBH_4$, produces mostly single-crystal Au seed as reported by several research groups [3, 27, 28]. Figure 1 shows 3–5 nm-sized single-crystalline Au NP seeds obtained from the first reaction step. The inset in Fig. 1 shows the atomistic model of single-crystal Au NP [26]. The formation of these Au nanocrystal seeds constitutes the most important step during NP synthesis, as the structure of these seeds directly affects the shape of final NPs.

Larger Au NPs shown in Fig. 2 were formed via the heterogeneous seed-mediated nucleation and growth during the second step of reaction. Here the NPs appear to have uniform shapes with the majority of them being of $\sim 12 \pm 1$ nm in size and exhibiting octahedral morphology bounded by (100) and (111) faces, with the occasional formation of triangle-shaped NPs [3, 27]. The higher-magnification STEM micrograph, along with the atomistic model for Au octahedral NP, is shown in the inset of Fig. 2.

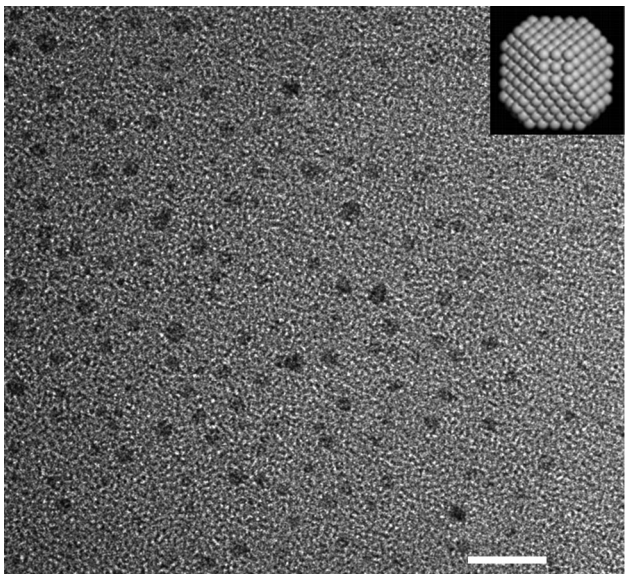

Fig. 1 TEM micrograph of single-crystal Au seed with the sizes ranging 3–5 nm. *Inset* shows the atomistic model for the single-crystal Au seed. *Scale bar* 20 nm

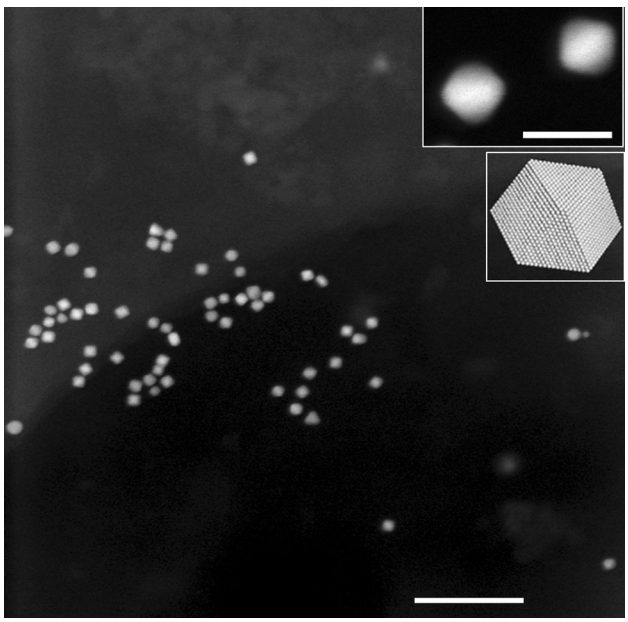

Fig. 2 STEM micrograph of Au octahedral NPs ~12 nm grown from single-crystal Au seeds as presented in Fig. 1. Figure *inset* shows the magnified Au nanocrystals along with the atomistic model for octahedral Au NPs. *Scale bar* 100 nm; *inset scale bar* 20 nm

During the next step of the reaction, where the octahedral Au NPs are incubated with the Pd precursor and reduced by AA, the epitaxial growth of Pd takes place on the surface of Au NPs and core–shell structures are formed. Figure 3 shows the low magnification STEM micrograph of the prepared Au–Pd core–shell NPs. The majority of these particles are nanocubes, with occasionally observed triangular particles. The majority of these particles are nanocubes of $\sim 20 \pm 1$ nm in size, with occasionally observed triangular particles of $\sim 30 \pm 3$ nm in size. Working with the HAADF-STEM utilizes the so-called *Z*-contrast and allows facile differentiation between the NP core (Au) and shell (Pd) of the produced Au–Pd nanostructures. It is clearly seen from the HAADF-STEM image in Fig. 3 that the strongly scattering core contains the element with a higher atomic number (Au), while the shell is comprised the element with a lower atomic number (Pd). The lattice constant for Au is 4.08 Å and for Pd is 3.89 Å, with lattice mismatch 4.8%, inferring the likelihood of the epitaxial growth of Pd over Au forming core–shell NPs [27, 29, 30]. According to Tsuji et al., the lattice mismatch between Au and Pd is below 5%, facilitating the epitaxial growth along all directions [31]. Upon adding Pd precursor, the nanocubes form from octahedral Au NPs via a more rapid growth of Pd along ⟨111⟩ direction as compared to that along ⟨100⟩ direction from the epitaxial growth of Pd over Au [26, 27, 32]. This can be explained by the presence of the CTAB bilayer bound to the (100) surfaces of the octahedral Au NPs and inhibiting the growth along those directions, as reported by Rodriguez-Fernandez et al. [32].

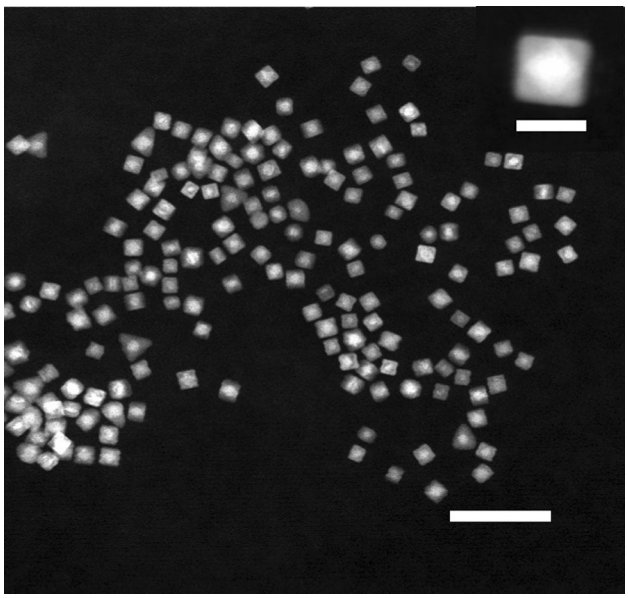

Fig. 3 STEM micrograph of Au–Pd core–shell nanocubes ~20 nm size with Au in the core and Pd in the shell. The typical Au–Pd core–shell nanocube in the *inset* shows that the core is made from Au (higher contrast) and the shell is made from Pd (lower contrast). *Scale bar* 100 nm; *inset scale bar* 20 nm

The schematics of the reaction pathway to the formation of multilayered core–shell Au–Pd–Au NP are presented in Fig. 4. The single-crystal Au seeds are grown into the octahedral Au NPs. Addition of the Pd precursor followed by the reduction with a mild reducing agent AA leads to the epitaxial growth of Pd onto Au core, to form the initial core–shell structures, mainly nanocubes. On the other hand, the singly twinned Au seeds grow into triangular-like structures, and the reduction of added Pd precursor with AA leads to the formation of core–shell triangular NPs, as described by Jose-Yacaman and coworkers [26]. Following the previous reports on DNA-mediated NP growth [23, 24, 33], upon the addition of T30 DNA to the reaction flask, the DNA molecules undergo hybridization on the surface of Pd nanocubes. The growth is determined by the binding affinity of DNA to the Pd surface as reported by Song et al. The binding affinity of T30 DNA is weaker [34] and will bind to lower energy facets in AuPd core–shell nanocube. The growth is initiated along {100} facets for the formation of {111} facets, resulting the changes in morphology from nanocube to nanostar-like morphology [35]. The zeta potential measurements, reported by Pallares et al. [36], imply the binding affinity of T30 DNA to AuPd core–shell NPs. Upon the final reduction of gold precursor, the outer layer Au is formed on the top of Pd shell. The use of DNA leads to the formation of the nanostar-like shape, and the presence of excess Au results in a hexagonal platelet comprised Au core, intermediate Pd shell, and Au outer shell. It is worth noting, that by the ultimate morphology, size, and thickness of the resultant NPs can be controlled by adjusting the concentration of the reagents. A control experiment carried out in the absence of DNA, Au layers were formed on the shell of Au–Pd core–shell nanocube without affecting the initial morphology of Au–Pd particles. Evidently, the distinct difference in the morphology of the resultant NPs obtained in the synthesis is associated solely with the presence of DNA.

The HAADF-STEM micrograph of three-layered Au–Pd–Au core–shell NPs obtained from the Au–Pd core–shell nanocubes in the presence of T30 DNA is presented in Fig. 5(a). Here the STEM micrograph reveals the presence of hexagonal platelets, apparently forming from the intermediate 6-cornered nanostars. The nanostars are represented by dotted white circles in Fig. 5(a), while the hexagonal platelets are represented by solid red circles. The reduction of excess Au precursor and deposition into the nanostars led to the formation of hexagonal platelets. Although the morphology of the resultant hexagonal platelets is homologous with the intermediate pointed star-like shape, the size of the particles ranges from ~24 to ~52 nm. The size distribution of synthesized NP is inset in

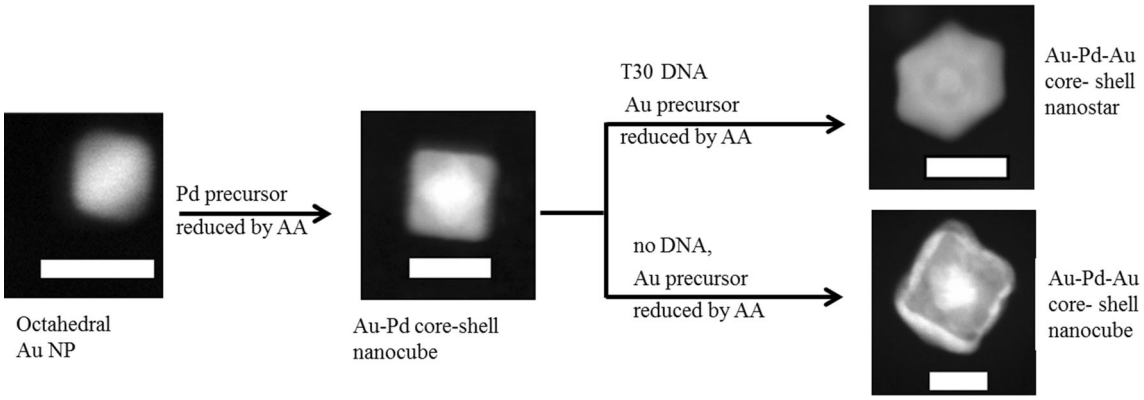

Fig. 4 Shape modification using DNA. AuPd core–shell nanocube is transformed into star-like AuPdAu core–shell particles using T30 DNA, while the shape remains unchanged in the absence of DNA, *scale bar* 20 nm

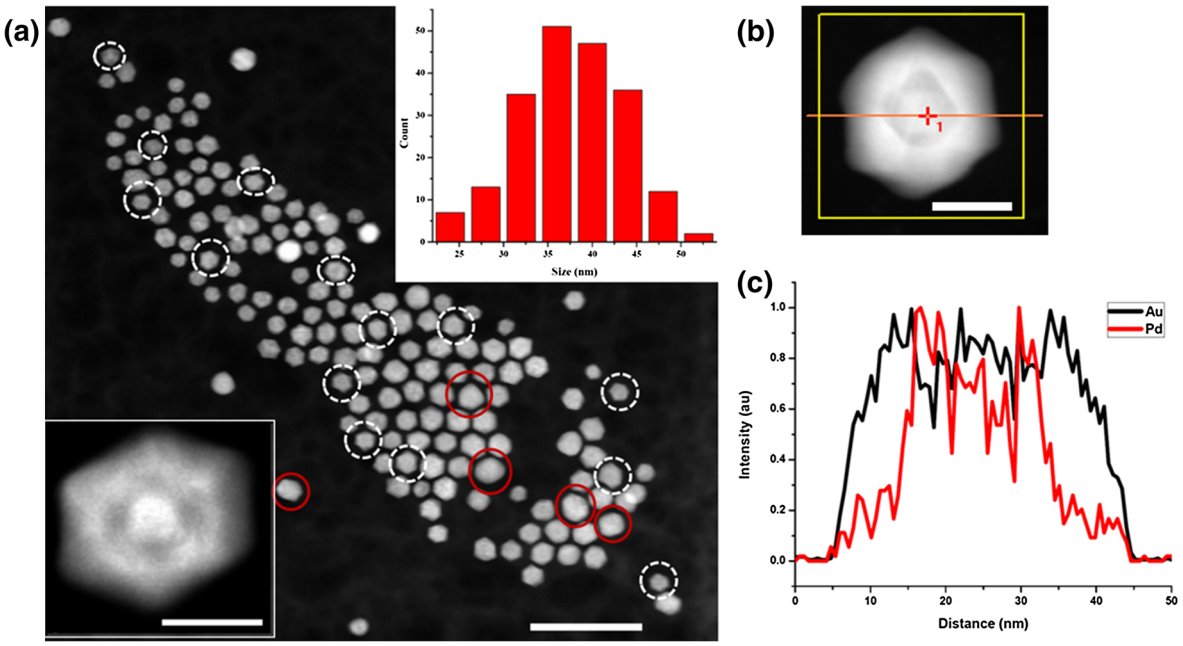

Fig. 5 (**a**) HAADF-STEM micrograph of Au–Pd–Au multilayered core–shell nanostructures obtained using T30 DNA molecules with the size distribution shown in the *inset*. The most interesting feature is the shape change from cubic to this structure. The majority of nanoparticles are nanostars, as highlighted by *white dotted circles*, with some of them well-developed hexagonal platelet-like structures denoted by *red solid circles*. During the growth process, the presence of excess amount of Au leads to the formation of hexagonal platelets structures. Lower-left *inset* in (**a**) shows typical nanostar with Au core, Pd intermediate shell, and outer Au shell regions. (**b**) Position of the line profile scan and (**c**) drift-corrected EDS line profile acquired from (**b**). EDS line profile analysis confirms the presence of Au in outer shell, Pd in intermediate shell, and Au in the inner core, thus proving the presence of multilayered AuPdAu core–shell structures. *Scale bar*: 200 nm; *inset scale bar* and (**b**): 20 nm

Fig. 5(a) for more than 200 particles. The inset shows that 90% of the particle size range from 30 to 45 nm, with 10% of the particles being smaller than 30 nm or larger than 45 nm sizes. The introduction to the reaction of T30 DNA leads to formation of substantially thicker hexagonal multilayered nanostructures with preferential growth along some directions forming the asymmetrical shapes. The growth mechanisms of anisotropic NPs using DNA remain a focus of intense research. Recently, Song et al. showed that the growth in such a reaction is determined by the binding affinity of DNA with the corresponding facets [35]. The stronger binding affinity of DNA results in lesser growth of particles along that direction, while the weaker binding affinity of DNA leads to a more pronounced growth along that direction. Since the T30 DNA used in this work has, reportedly, weaker binding affinity and facilitates the formation of lower energy {111} facets [34, 35], leading to the formation of anisotropic nanostars. The

resultant three-layered particles clearly exhibit 6-pointed corners, pointing to a prevalent specific growth mechanism. Notably, while the bimetallic Au–Pd NPs show a minor fraction of triangular particles, the three-la Au–Pd–Au NPs exhibit 6-pointed star-like morphology almost exclusively. It is worth noting that the effect of the DNA appears to be more pronounced in nanocubes, as compared to that observed in triangular particles, as seen from the shape transformation. One possible reason for this might be associated with the presence of a higher number of corners in nanocubes as compared to the triangular NPs. From the higher-magnification HAADF-STEM image of magnified NP (inset in Fig. 5a), the presence of three layers can be inferred: these are the inner region (core) Au with a strong contrast, the middle region (intermediate shell) with the weaker-scattering Pd, and the outer shell layer comprised the stronger-contrast Au. These unusual structures provide the insight into the morphology transformation in NPs with multilayered structures. The localized chemical information of the multilayered core–shell NP is investigated using energy dispersive x-ray spectroscopy (EDS) line profile scan. The EDS line profile of a nanostar in Fig. 5(b) is presented in Fig. 5(c). This line profile (Fig. 5c) reveals the local mapping along the scanned line, confirming the presence of Au in outermost shell region, Pd in intermediate shell region, and Au in the core region.

The HAADF-STEM micrographs for Au–Pd–Au multilayered core–shell NPs obtained without DNA are presented in Fig. 6. As in the previous case, the *Z*-contrast images show that the core is made from Au, intermediate layer is made from Pd, and outer shell is again made from Au. The size of the particles ranges from 35 to 45 nm, with very thin layers ($\sim 3 \pm 1$ nm) of outer Au shell. It should be noted that in the absence of DNA, formation of outer gold shell occurs in a symmetric, isotropic manner, whereas in the presence of DNA gold shell exhibits some direction-specific, preferential growth. The shape of core–shell nanocube, unaltered by the addition of outer Au shell region, is distinctly different from that of the Au–Pd–Au NP obtained in the presence of DNA presented in Fig. 5. The formation of multi-shell core–shell structures in the absence of DNA is in good agreement with the previous reports by Li et al. and Wang et al. [37, 38].

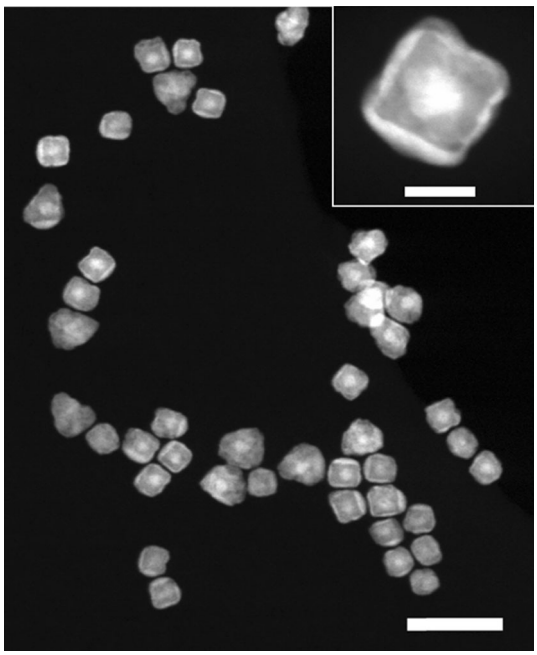

Fig. 6 HAADF-STEM images for AuPdAu multilayered core–shell NPs obtained in the absence of T30 DNA. The inner core is Au, intermediate shell is Pd and outer shell is again Au as seen from different contrast. The typical structure is *inset* in figure showing the stronger-contrast Au and weaker contrast Pd. The *scale bar* is 100 nm for main frame and 20 nm for *inset image*

Conclusions

In this report, we presented the modification in morphology of Au–Pd bimetallic core–shell nanocubes into multilayered core–shell nanostars with 6 corners and finally into hexagonal platelets-like structures, using T30 DNA molecules, effectively controlling the morphology and size of the bimetallic NPs. It was hypothesized that the T30 DNA molecules hybridize to the surface of Au–Pd core–shell nanocubes, and the growth is directed by the binding affinity of T30 DNA. The weaker binding affinity of T30 DNA directs the growth to favor the formation of lower energy {111} facets resulting the changes in morphology from nanocubes to nanostar. During the reduction with AA, the growth of the particle shell proceeds along the selected directions dictated by the template, in this case leading to formation of star-like nanostructures with 6 corners. The growth might also be from the uneven growth of particles resulting from the hybridization of DNA molecules onto the Pd surface. In the absence of DNA molecules, multiple-layered core–shell Au–Pd–Au nanocubes were formed without altering the morphology of the Au–Pd nanocubes, similar to reports by Li et al. and Wang et al. [37, 38]. The local chemical environment in the multi-shell NPs was probed using EDS line scan. The ability to tune different shapes, size, and crystalline structure will broaden the application of such NPs. Hence, the ability to synthesize the core–shell bimetallic NPs with desired shape and controlled deposition of different metals with multi-shells will be an important step toward designing the heterometallic NPs with novel properties arising from the synergetic combination of presence of multiple shells with different layers and metals.

Acknowledgments T.P. acknowledges support from the Department of Energy Office of Science Early Career Research Award,

Biomolecular Materials Program. This work was supported by the U.S. Department of Energy, Office of Basic Energy Science, Division of Materials Sciences and Engineering. The research was performed at the Ames Laboratory, which is operated for the U.S. Department of Energy by Iowa State University under Contract No. DE-AC02-07CH11358. The authors are very grateful to the laboratory of Prof. Yi Lu from University of Illinois, Urbana, for providing the T30 DNA molecules used for this synthesis and for useful discussions.

References

1. M.R. Buck, J.F. Bondi, R.E. Schaak, A total-synthesis framework for the construction of high-order colloidal hybrid nanoparticles. Nat. Chem. **4**, 37 (2012)
2. C. Burda, X. Chen, R. Narayanan, M.A. El-Sayed, Chemistry and properties of nanocrystals of different shapes. Chem. Rev. **105**, 1025 (2005)
3. Y. Xia, Y. Xiong, B. Lim, S.E. Skrabalak, Shape-controlled synthesis of metal nanocrystals: simple chemistry meets complex physics? Angew. Chem. Int. Ed. **48**, 60 (2009)
4. S.A. Maier, M.L. Brongersma, P.G. Kik, S. Meltzer, A.A. Requicha, H.A. Atwater, Plasmonics—a route to nanoscale optical devices. Adv. Mater. **13**, 1501 (2001)
5. S.E. Skrabalak, L. Au, X. Lu, X. Li, Y. Xia, Gold nanocages for cancer detection and treatment. Fut. Med. **2**, 657–668 (2007)
6. E. Pérez-Tijerina, M.G. Pinilla, S. Mejia-Rosales, U. Ortiz-Méndez, A. Torres, M. José-Yacamán, Highly size-controlled synthesis of Au/Pd nanoparticles by inert-gas condensation. Faraday Disc. **138**, 353 (2008)
7. C. Kiely, Electron microscopy: new views of catalysts. Nat. Mater. **9**, 296 (2010)
8. J. Xu, A.R. Wilson, A.R. Rathmell, J. Howe, M. Chi, B.J. Wiley, Synthesis and catalytic properties of Au–Pd nanoflowers. ACS Nano **5**, 6119 (2011)
9. J.W. Hong, D. Kim, Y.W. Lee, M. Kim, S.W. Kang, S.W. Han, Atomic-distribution-dependent electrocatalytic activity of Au–Pd bimetallic nanocrystals. Angew. Chem. **123**, 9038 (2011)
10. C.-W. Yang, K. Chanda, P.-H. Lin, Y.-N. Wang, C.-W. Liao, M.H. Huang, Fabrication of Au–Pd core–shell heterostructures with systematic shape evolution using octahedral nanocrystal cores and their catalytic activity. J. Am. Chem. Soc. **133**, 19993 (2011)
11. C.-L. Lu, K.S. Prasad, H.-L. Wu, J.-A.A. Ho, M.H. Huang, Au nanocube-directed fabrication of Au–Pd core–shell nanocrystals with tetrahexahedral, concave octahedral, and octahedral structures and their electrocatalytic activity. J. Am. Chem. Soc. **132**, 14546 (2010)
12. L. Zhang, J. Zhang, Q. Kuang, S. Xie, Z. Jiang, Z. Xie, L. Zheng, Cu^{2+}-assisted synthesis of hexoctahedral Au–Pd alloy nanocrystals with high-index facets. J. Am. Chem. Soc. **133**, 17114 (2011)
13. D. Ferrer, A. Torres-Castro, X. Gao, S. Sepulveda-Guzman, U. Ortiz-Mendez, M. Jose-Yacaman, Three-layer core/shell structure in Au-Pd bimetallic nanoparticles. Nano Lett. **7**, 1701 (2007)
14. R. Ferrando, J. Jellinek, R.L. Johnston, Nanoalloys: from theory to applications of alloy clusters and nanoparticles. Chem. Rev. **108**, 845 (2008)
15. B. Sacca, C.M. Niemeyer, Functionalization of DNA nanostructures with proteins. Chem. Soc. Rev. **40**, 5910 (2011)
16. A. Stadler, C. Chi, D. van der Lelie, O. Gang, DNA-incorporating nanomaterials in biotechnological applications. Nanomedicine **5**, 319 (2010)
17. A. Kumar, J.-H. Hwang, S. Kumar, J.-M. Nam, Tuning and assembling metal nanostructures with DNA. Chem. Comm. **49**, 2597 (2013)
18. L.-L. Li, P. Wu, K. Hwang, Y. Lu, An exceptionally simple strategy for DNA-functionalized up-conversion nanoparticles as biocompatible agents for nanoassembly, DNA delivery, and imaging. J. Am. Chem. Soc. **135**, 2411 (2013)
19. M. Mertig, L. Colombi-Ciacchi, R. Seidel, W. Pompe, A. De Vita, DNA as a selective metallization template. Nano Lett. **2**, 841 (2002)
20. S. Helmi, C. Ziegler, D.J. Kauert, R. Seidel, Shape-controlled synthesis of gold nanostructures using DNA origami molds. Nano Lett. **14**, 6693 (2014)
21. G. Tikhomirov, S. Hoogland, P. Lee, A. Fischer, E.H. Sargent, S.O. Kelley, DNA-based programming of quantum dot valency, self-assembly and luminescence. Nat. Nanotechnol. **6**, 485 (2011)
22. Z. Wang, J. Zhang, J.M. Ekman, P.J. Kenis, Y. Lu, DNA-mediated control of metal nanoparticle shape: one-pot synthesis and cellular uptake of highly stable and functional gold nanoflowers. Nano Lett. **10**, 1886 (2010)
23. L.H. Tan, H. Xing, Y. Lu, DNA as a powerful tool for morphology control, spatial positioning, and dynamic assembly of nanoparticles. Acc. Chem. Res. **47**, 1881 (2014)
24. Z. Wang, L. Tang, L.H. Tan, J. Li, Y. Lu, Discovery of the DNA "genetic code" for abiological gold nanoparticle morphologies. Angew. Chem. Int. Ed. **51**, 9078 (2012)
25. N. Bhattarai, G. Casillas, A. Ponce, M. Jose-Yacaman, Strain-release mechanisms in bimetallic core–shell nanoparticles as revealed by Cs-corrected STEM. Surf. Sci. **609**, 161 (2013)
26. N. Bhattarai, G. Casillas, S. Khanal, J.J.V. Salazar, A. Ponce, M. Jose-Yacaman, Origin and shape evolution of core–shell nanoparticles in Au–Pd: from few atoms to high Miller index facets. J. Nanopart. Res. **15**, 1 (2013)
27. Y. Ding, F. Fan, Z. Tian, Z.L. Wang, Atomic structure of Au–Pd bimetallic alloyed nanoparticles. J. Am. Chem. Soc. **132**, 12480 (2010)
28. M.H. Huang, P.H. Lin, Shape-controlled synthesis of polyhedral nanocrystals and their facet-dependent properties. Adv. Funct. Mater. **22**, 14 (2012)
29. J. Zhang, Y. Tang, K. Lee, M. Ouyang, Nonepitaxial growth of hybrid core-shell nanostructures with large lattice mismatches. Science **327**, 1634 (2010)
30. P. Reiss, M. Protiere, L. Li, Core/shell semiconductor nanocrystals. Small **5**, 154 (2009)
31. M. Tsuji, K. Ikedo, M. Matsunaga, K. Uto, Epitaxial growth of Au@ Pd core–shell nanocrystals prepared using a PVP-assisted polyol reduction method. Cryst. Eng. Commun. **14**, 3411 (2012)
32. J. Rodríguez-Fernández, J. Pérez-Juste, P. Mulvaney, L.M. Liz-Marzán, Spatially-directed oxidation of gold nanoparticles by Au(III)-CTAB complexes. J. Phys. Chem. B **109**, 14257 (2005)
33. J. Liu, J. Liu, L. Yang, X. Chen, M. Zhang, F. Meng, T. Luo, M. Li, Nanomaterial-assisted signal enhancement of hybridization for DNA biosensors: a review. Sensors **9**, 7343 (2009)
34. H. Kimura-Suda, D.Y. Petrovykh, M.J. Tarlov, L.J. Whitman, Base-dependent competitive adsorption of single-stranded DNA on gold. J. Am. Chem. Soc. **125**, 9014 (2003)
35. T. Song, L. Tang, L.H. Tan, X. Wang, N.S.R. Satyavolu, H. Xing, Z. Wang, J. Li, H. Liang, Y. Lu, DNA-encoded tuning of geometric and plasmonic properties of nanoparticles growing from gold nanorod seeds. Angew. Chem. Int. Ed. **54**, 8114 (2015)
36. R.M. Pallares, S.L. Kong, T.H. Ru, N.T. Thanh, Y. Lu, X. Su, A plasmonic nanosensor with inverse sensitivity for circulating cell-free DNA quantification. Chem. Commun. **51**, 14524 (2015)
37. J. Li, Y. Zheng, J. Zeng, Y. Xia, Controlling the size and morphology of Au@ Pd core-shell nanocrystals by manipulating the kinetics of seeded growth. Chemistry A **18**, 8150 (2012)
38. F. Wang, L.D. Sun, W. Feng, H. Chen, M.H. Yeung, J. Wang, C.H. Yan, Heteroepitaxial growth of core–shell and core–multi-shell nanocrystals composed of palladium and gold. Small **6**, 2566 (2010)